CrystEngComm

ROYAL SOCIETY OF CHEMISTRY

PAPER

View Article Online
View Journal | View Issue

Cite this: *CrystEngComm*, 2020, **22**, 6152

Selective encapsulation and extraction of hydrogenphosphate by a hydrogen bond donor tripodal receptor†

Sandeep Kumar Dey, *[a] Archana,[a] Sybil Pereira,[a] Sarvesh S. Harmalkar,[a] Shashank N. Mhaldar,[a] Vivekanand V. Gobre[a] and Christoph Janiak [b]

Selective encapsulation of an anion by a hydrogen bond donor scaffold demands design and synthesis of suitable receptors which could discriminate between anions of identical size and shape or basicity. Here, we report the anion coordination chemistry of two second generation tripodal receptors (**AUL** and **AAL**) based on ^{1}H-NMR and crystallization experiments. The tripodal urea-based receptor **AUL** can selectively encapsulate a hydrogenphosphate (HPO_4^{2-}) dianion by six strong hydrogen bonds donated from the three urea groups. Theoretical calculations showed that **AUL** has the highest binding affinity for hydrogenphosphate when compared to other competitive anions (F^-, CN^-, CH_3COO^- and HSO_4^-). Because of its HPO_4^{2-} selectivity, **AUL** has been successfully employed in the extraction of HPO_4^{2-} from water in the presence of competitive anions (F^-/OH^-/CH_3COO^-) by anion exchange between two immiscible phases. On the other hand, the tripodal amide-based receptor **AAL** when crystallized in the presence of F^-, CN^-, CH_3COO^-, $H_2PO_4^-$ and HSO_4^- did not yield any hydrogen-bonded receptor–anion complex and instead crystalline **AAL** was precipitated in each case. ^{1}H-NMR experiments showed significant broadening and/or downfield shift of –NH signals in **AUL** and **AAL** upon additions of F^-, Cl^-, CN^-, CH_3COO^- and $H_2PO_4^-$ (supplied as tetraalkylammonium salts), indicative of strong hydrogen bonding interactions between –NH donors and anions in the solution-state.

Received 9th June 2020,
Accepted 6th August 2020

DOI: 10.1039/d0ce00834f

rsc.li/crystengcomm

Introduction

Anion coordination chemistry has already evolved into an established and recognized field of research within the realm of supramolecular chemistry over the past three decades.[1] Hydrogen bond donor (HBD) acyclic and macrocyclic receptors have been widely studied in solution and solid states where the receptor–anion binding constants and X-ray structures of hydrogen bonded anion complexes were determined, respectively.[2] Several HBD receptors which can selectively or preferentially bind a specific anion (halide/oxo-anion) are reported in the literature.[3] The anion selectivity of a receptor is largely governed by the receptor–anion complementarity where the acidity of the hydrogen bond donor groups and basicity of an anion plays a key role in the formation of a stable hydrogen bonded anion complex. For macrocyclic and tripodal receptors, both the cavity size and nature of the hydrogen bond donor groups determine the anion selectivity, although discrimination between anions of similar basicity (such as F^-, CH_3COO^-, HCO_3^-) or anions of identical shape and size (such as SO_4^{2-}, HPO_4^{2-}, $HAsO_4^{2-}$) can be challenging to achieve. Conformational flexibility in the receptor molecule often allows coordination of anions of different geometries (spherical, planar and tetrahedral) by structural reorganization as exemplified by several tripodal urea/thiourea receptors.[4] Nonetheless, a few urea/thiourea based tripodal receptors among others are known to preferentially coordinate to a specific anion over some other anions and thus selective separation of anions has been achieved by liquid–liquid extraction or crystallization experiments in a competitive environment.[5]

Selective removal of inorganic phosphate anions ($H_2PO_4^-$, HPO_4^{2-} and PO_4^{3-}) from freshwater ecosystems contaminated with agricultural and household run offs containing fertilizers and detergents is crucial in limiting eutrophication of natural water bodies.[6] However, due to the high Gibbs hydration free energies of phosphates (ΔG_H of $H_2PO_4^- < HPO_4^{2-} < PO_4^{3-}$)[7] and the presence of other competitive

[a] *School of Chemical Sciences, Goa University, Taleigao Plateau, Goa 403206, India. E-mail: sandeepdey@unigoa.ac.in; Tel: +91 7387633550*
[b] *Institute for Inorganic and Structural Chemistry, Heinrich-Heine University Dusseldorf, 40225 Dusseldorf, Germany. E-mail: janiak@uni-duesseldorf.de; Tel: +49 8669609302*

† Electronic supplementary information (ESI) available: Synthesis details, characterization data, ^{1}H-NMR experiments with quaternary ammonium salts, DFT optimized structures and powder XRD patterns. CCDC 2008261–2008263. For ESI and crystallographic data in CIF or other electronic format see DOI: 10.1039/d0ce00834f

anions (Cl^-, NO_3^- and SO_4^{2-}) in freshwater bodies, selective phosphate removal is a challenging task. Thus, development of synthetic HBD receptors capable of selective encapsulation and separation of inorganic phosphates is crucial due to their diverse biological and environmental relevance.[8] Over the past two decades, many researchers have devoted themselves to developing artificial receptors for the selective binding of phosphates *via* non-covalent interactions, featuring different topological complementarities for the anion.[9]

Herein, we report selective encapsulation of the hydrogenphosphate dianion (HPO_4^{2-}) by a tripodal urea-based receptor **AUL** (Scheme 1) and subsequent extraction of the oxo-anion from water in the presence of highly competitive anions. Our experimental results showed that the urea-based receptor **AUL** can selectively form a hydrogen bonded complex with hydrogenphosphate [$(n\text{-}Bu_4N)_2$(**AUL**·HPO_4)·DMSO·CH_3CN], while the **AUL**·2DMSO adduct was formed in the presence of other competitive anions such as F^-, Cl^-, CN^-, CH_3COO^- and HSO_4^- under identical crystallization conditions. Theoretical binding energy calculations were found to be in agreement with the experimental results showing the highest binding affinity of **AUL** for HPO_4^{2-} in the energy optimized receptor–anion complexes. On the other hand, the amide-based receptor **AAL** (Scheme 1) when crystallized in the presence of different anions such as F^-, Cl^-, CN^-, CH_3COO^- and $H_2PO_4^-$ did not form an anion complex. Instead, crystalline **AAL** formed in each case suggesting that **AAL** is not a suitable anion receptor. Solution state anion binding studies of **AUL** and **AAL** have also been carried out by ^{1}H-NMR spectroscopy with quaternary ammonium salts of different anions.

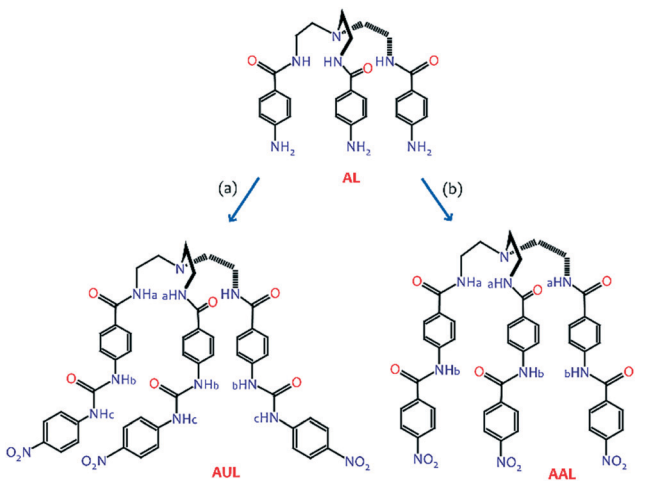

Scheme 1 Molecular structures of tripodal receptors **AUL** (urea-based) and **AAL** (amide-based) as synthesized from tris(4-amino-*N*-ethylbenzamide)amine **AL** by reaction with (a) 3.2 equivalents of 4-nitrophenyl isocyanate in dimethyl sulfoxide (DMSO), and (b) 3.5 equivalents of 4-nitrobenzoyl chloride in the tetrahydrofuran–ethanol solvent mixture (8 : 2 v/v) in the presence of 2 equivalents of tetrabutylammonium chloride. –NH protons of the receptors are labelled a, b and c to discuss their relevance in ^{1}H-NMR experimental discussions in the text (synthesis details are provided in the ESI†).

Numerous tris(2-aminoethyl)amine (Tren)-based tripodal tris-urea/thiourea and tris-amide receptors have been studied for anion coordination,[4] among which only a few receptors are known to selectively coordinate to a specific anion (Scheme 2a).[3a–f] Synthesized from nitrophenyl functionalized tripodal tris-urea receptors, Biao Wu *et al.* have reported a series of tripodal hexa-urea receptors which showed preferential binding of sulfate in the receptor cavity (Scheme 2b).[10] To tune the anion selectivity in tripodal receptors, we have synthesized two Tren-based receptors both having an identical inner amide cavity but differing in their outer HBD cavities. Receptor **AUL** has an outer tris-urea cavity and **AAL** has an outer tris-amide cavity. Anion coordination by tripodal receptors having an inner tris-amide cavity and an outer tris-urea cavity has not been studied before. **AAL**, a hexa-amide receptor, can be considered as the amide analogue of the hexa-urea receptor (6c in Scheme 2b) that was observed to encapsulate a sulfate anion exclusively in the inner tris-urea cavity only.

Results and discussion

In our effort to achieve selective anion binding, we have synthesized two second generation tripodal receptors (**AUL**

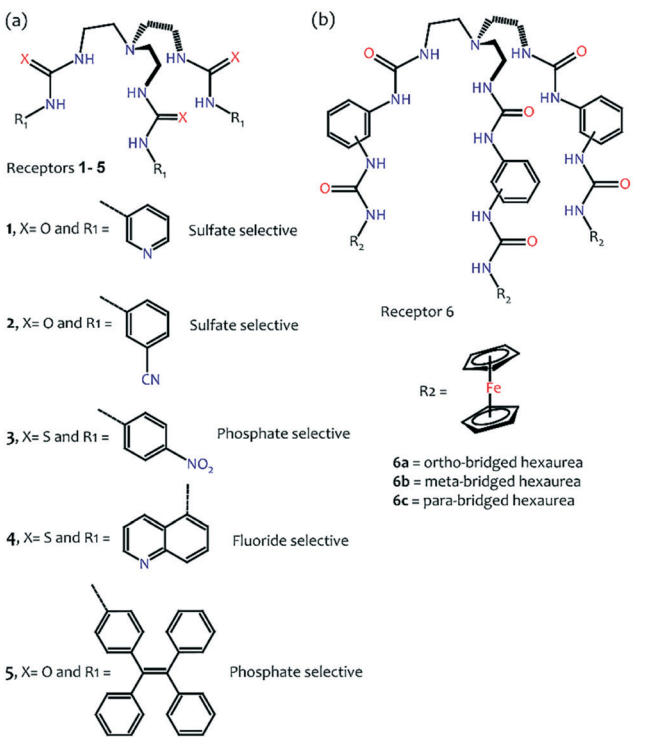

Scheme 2 (a) Tren-based tripodal tris-urea/thiourea receptors (**1**–**5**) known for selective recognition of sulfate (SO_4^{2-}), phosphate (PO_4^{3-}) and fluoride (F^-) ions,[3a–e] (b) Tren-based tripodal hexa-urea receptors (**6a**–**c**) for recognition of a sulfate (SO_4^{2-}) ion;[10] *ortho*-bridged hexa-urea **6a** could encapsulate a SO_4^{2-} ion within the complementary receptor cavity, meta-bridged hexa-urea **6b** could encapsulate two SO_4^{2-} ions within the inner and outer tris-urea cavities, and *para*-bridged hexa-urea **6c** could encapsulate a SO_4^{2-} ion within the inner tris-urea cavity only.

and **AAL**) by post-synthetic modification of tris(4-nitro-*N*-ethylbenzamide)amine, (see section S2a in the ESI†), which is a Tren-based tris-amide receptor with a peripheral nitrophenyl ring.[11] Tris(4-nitro-*N*-ethylbenzamide)amine was reduced to its amine analogue tris(4-amino-*N*-ethylbenzamide)amine **AL** (Scheme 1) which was then then reacted with 4-nitrophenyl isocyanate and 4-nitrobenzoyl chloride to obtain **AUL** and **AAL**, respectively (see sections S2b and S2c in the ESI†). The tripodal receptors **AUL** and **AAL** were characterized by ^{1}H-NMR, ^{13}C-NMR, FT-IR (KBr) and X-ray diffraction techniques. Both receptors are soluble in DMSO and DMF, but insoluble in other organic solvents such as chloroform, acetonitrile, tetrahydrofuran and methanol/ethanol. The solution state anion binding properties of **AUL** and **AAL** were investigated by ^{1}H-NMR spectroscopy in DMSO-d_6 and crystallization experiments in the DMSO–acetonitrile (8 : 2 v/v) mixture were performed to establish the formation of hydrogen-bonded anion complexes in the solid state. In a typical qualitative ^{1}H-NMR experiment, 15 mg of **AUL**/**AAL** was dissolved in 0.6 ml of DMSO-d_6 and 2 to 4 equivalents of tetrabutylammonium (n-Bu_4N^+) or tetraethylammonium (Et_4N^+) salt (halide/oxyanion) were added into the solution.[12] The solution was then sonicated to ensure complete solubility of the receptor and added salt in DMSO-d_6 before ^{1}H-NMR analysis.

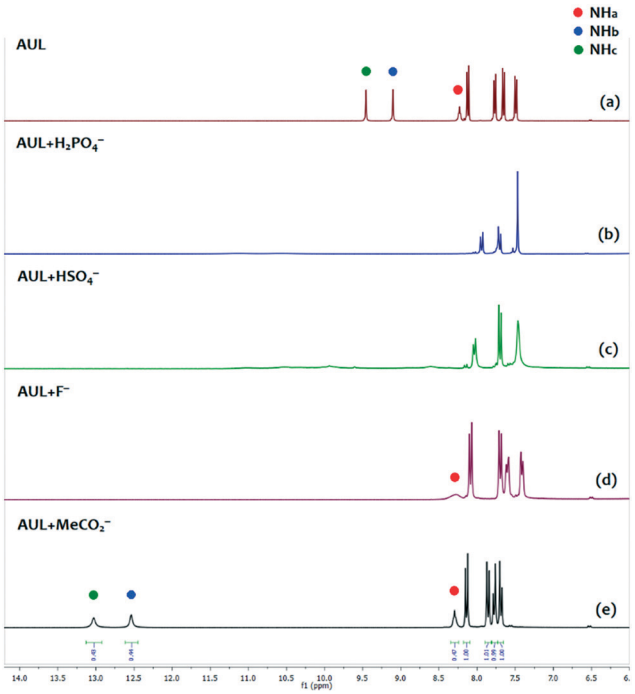

Fig. 1 Aromatic region (6–14 ppm) of ^{1}H-NMR (DMSO-d_6) spectra of (a) **AUL** and in the presence of (b) (n-Bu_4N^+)$H_2PO_4^-$, (c) (n-Bu_4N^+)HSO_4^-, (d) (n-Bu_4N^+)F^- and (e) $Li^+CH_3COO^-$ (full spectra are provided in Fig. S11–S14 in the ESI†).

Anion binding studies of urea-based receptor AUL

Urea –NH protons are potential hydrogen bond donors and known to form strong hydrogen bonds with halides and oxo-anions.[4] The ^{1}H-NMR spectrum of **AUL** in DMSO-d_6 showed the amide –NH_a signal at 8.23 ppm and the urea –NH protons appeared at 9.10 and 9.46 ppm for –NH_b and –NH_c, respectively (Fig. 1a). Urea –NH_c bonded to the nitrophenyl ring is more downfield shifted (9.46 ppm) as compared to –NH_b bonded to the inner benzamide ring (9.10 ppm) because the peripheral nitrophenyl ring is more electron deficient than the inner benzamide ring. Aromatic –CH proton signals appeared as doublets due to *para* substitution of the aromatic rings.

Addition of tetrabutylammonium (n-Bu_4N^+) salts of F^-, HSO_4^- and $H_2PO_4^-$ to solutions of **AUL** (in DMSO-d_6) resulted in disappearance of urea –NH signals due to hydrogen bond formation between the –NH protons and the negatively charged ions (Fig. 1b–d). Strong hydrogen bonds between –NH protons and an anion often lead to shifts in ^{1}H-NMR signals. At the same time, dynamic anion coordination *i.e.*, if the exchange of a complexed and an uncomplexed guest (anion) is within the NMR time scale, significant peak broadening up to the point of disappearance of the signal occurs.[13] Also, addition of lithium acetate resulted in the large downfield shift of urea –NH signals by 3.5 ppm with concomitant broadening, but still the presence of the singlet peaks (Fig. 1e) was observed.[14] Due to interaction of urea –NH protons with the anion, the electronic environment of the adjacent aromatic rings was affected and therefore, some changes in peak positions have also been observed for the aromatic –CH signals (Fig. 1). Similarly, addition of (Et_4N^+)

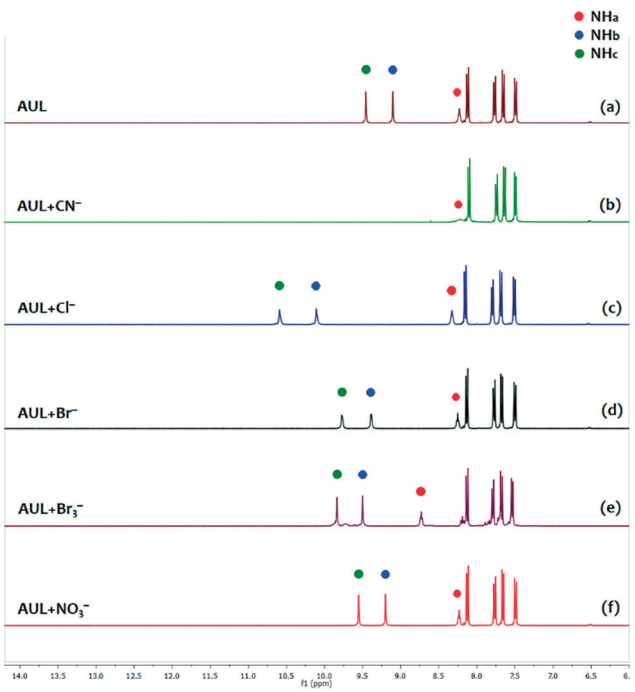

Fig. 2 Aromatic region (6–14 ppm) of ^{1}H-NMR (DMSO-d_6) spectra of (a) **AUL** and in the presence of (b) (Et_4N^+)CN^-, (c) (Et_4N^+)Cl^-, (d) (n-Bu_4N^+)Br^-, (e) (n-Bu_4N^+)Br_3^- and (f) (n-Bu_4N^+)NO_3^- (full spectra are provided in Fig. S16–S20 in the ESI†).

CN^- to a solution of **AUL** (in DMSO-d_6) showed disappearance of urea –NH signals due to hydrogen bond induced peak broadening, however with no observable changes in the –CH peak positions (Fig. 2b). Addition of chloride, bromide or tribromide salts showed a downfield shift of urea –NH peaks indicating receptor–anion interaction, but did not show any changes in the –CH peak positions. A considerable downfield shift of 1.0–1.1 ppm was observed for urea –NH signals, in the presence of $(Et_4N^+)Cl^-$ salt (Fig. 2c). However, $(n\text{-}Bu_4N^+)Br^-$ and $(n\text{-}Bu_4N^+)Br_3^-$ salt showed a downfield shift of 0.3–0.4 ppm for urea –NH signals indicative of weaker receptor–anion hydrogen bond interactions (Fig. 2d and e) as compared to chloride and fluoride. Finally, addition of $(n\text{-}Bu_4N^+)I^-$ or $(n\text{-}Bu_4N^+)NO_3^-$ showed negligible spectral changes of **AUL** in DMSO-d_6 (Fig. 2f).

Solution state anion binding studies showed strong hydrogen bond interactions of urea –NH protons with anions such as F^-, Cl^-, CN^-, CH_3COO^-, $H_2PO_4^-$ and HSO_4^- (Fig. 1 and 2). Thus, in order to obtain hydrogen-bonded anion complexes in the solid state, we have crystallized **AUL** in the presence of $n\text{-}Bu_4N^+$ or Et_4N^+ salts of the above anions. In a typical crystallization experiment, 100 mg of **AUL** was dissolved in 5 mL of DMSO–CH_3CN (8 : 2 v/v) solvent mixture and an excess of tetraalkylammonium salt (5 equivalents) was added into it followed by stirring at room temperature for about half an hour. The solution was then kept undisturbed at room temperature in a 10 mL beaker for crystallization upon evaporation.

In the crystallization experiments, from the solution mixtures of **AUL** with F^-, Cl^-, CH_3COO^-, CN^- or HSO_4^- only **AUL**·2DMSO could be crystallized (see below). Meanwhile, from the solution mixture of **AUL** with $H_2PO_4^-$, a hydrogen-bonded anion complex with composition $(n\text{-}Bu_4N)_2$(**AUL**·HPO_4)·DMSO·CH_3CN was crystallized (see below). Similar results have previously been observed for receptor **2** (Scheme 2) which formed a sulfate-encapsulated coordination polymer in the presence of Ag_2SO_4 (in water/acetone) and crystallization in the presence of other Ag^+ salts (NO_3^-, CH_3COO^-, $CH_3SO_3^-$ and BF_4^-) yielded crystals of **2**.[3b] ^{1}H-NMR spectra of the crystalline products obtained from the solution mixtures of **AUL** with F^-, Cl^-, CH_3COO^-, CN^- or HSO_4^- salts showed the absence of $(n\text{-}Bu_4N^+)/(Et_4N^+)$ signals in the aliphatic region and all five spectra closely resemble the ^{1}H-NMR spectrum of pure **AUL** recorded in DMSO-d_6. Only the ^{1}H-NMR spectrum of the crystals obtained from the solution mixture of **AUL** and $H_2PO_4^-$ showed the presence of tetrabutylammonium ($n\text{-}Bu_4N^+$) signals and a large downfield shift of urea –NH protons with concomitant broadening was observed (Fig. 4b and S21 in ESI†). The urea –NH signals were observed to appear at 11.90 and 13.10 ppm for $-NH_b$ and $-NH_c$, respectively (Fig. 4b). Changes in the peak position have also been observed for the aromatic –CH signals with respect to the **AUL** spectrum (Fig. 4a and b). The presence of $n\text{-}Bu_4N^+$ signals and the downfield shift of urea –NH protons indicate the possible coordination of a phosphate species by the urea-based receptor. Integration of the ^{1}H-NMR peaks

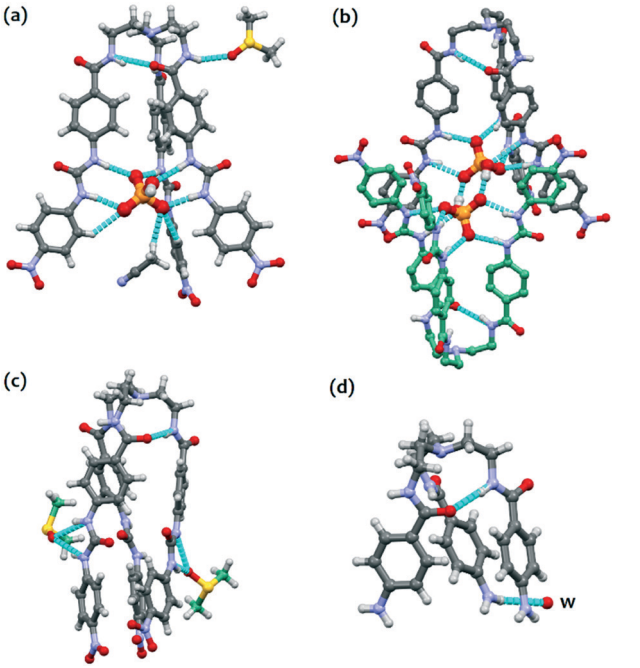

Fig. 3 Single crystal X-ray structures of (a) $(n\text{-}Bu_4N)_2$(**AUL**·HPO_4)·DMSO·CH_3CN showing receptor–anion hydrogen bonds, counter cations are not shown. (b) Dimeric capsular assembly formation in (n-$Bu_4N)_2$(**AUL**·HPO_4)·DMSO·CH_3CN where two receptor units are shown in different colors, counter cations, lattice solvents and CH protons are not shown for clarity of presentation. (c) **AUL**·2DMSO where DMSO carbon atoms are shown in different colors for clarity. (d) **AL**·H_2O where **W** represents lattice water. Hydrogen bonds are shown with blue dotted lines (see‡[1] footnote for crystal data). Color code: C = grey/green, N = blue, O = red, H = white, P = orange, and S = yellow.

suggests that there are at least two $n\text{-}Bu_4N^+$ cations present in the crystal structure, which implies that a HPO_4^{2-} dianion is coordinated to the urea groups. ^{31}P-NMR spectroscopy showed the appearance of a peak at 7.37 ppm which further suggested the presence of hydrogen-bonded HPO_4^{2-} in the crystal structure (Fig. S22 in the ESI†).[15] Thus, from the results of crystallization experiments it has been inferred that **AUL** is capable of forming a hydrogen-bonded complex with

‡ Single crystal data of $(n\text{-}Bu_4N)_2$(**AUL**·HPO_4)·DMSO·CH_3CN
CCDC No. 2008261, F = $C_{84}H_{127}N_{16}O_{17}PS$, M = 1696.05, T = 296(2) K, space group = $P\bar{1}$, a = 13.8359(11), b = 18.7145(15), c = 19.6641(15), α = 104.991(2)°, β = 99.589(3)°, γ = 104.672(2)°, V = 4608.9(6) Å^3, Z = 2, μ = 0.124 mm^{-1}, D = 1.221 g cm^{-3}, F(000) = 1818, reflections total = 19087, reflections gathered = 8892, R_{int} = 0.1148, $R_1(F)$ = 0.1055, w$R_2(F^2)$ = 0.2184, S = 1.018, N_{par} = 1085.
Single crystal data of **AUL**·2DMSO
CCDC No. 2008262, F = $C_{52}H_{57}N_{13}O_{14}S_2$, M = 1152.23, T = 100(2) K, space group = $P\bar{1}$, a = 9.4857(4), b = 17.0599(7), c = 18.6326(8), α = 64.282(2)°, β = 80.544(2)°, γ = 87.541(2)°, V = 2678.3(2) Å^3, Z = 2, μ = 0.180 mm^{-1}, D = 1.429 g cm^{-3}, F(000) = 1208, reflections total = 9430, reflections gathered = 8381, R_{int} = 0.0223, $R_1(F)$ = 0.0502, w$R_2(F^2)$ = 0.1355, S = 1.032, N_{par} = 773.
Single crystal data of **AL**·H_2O
CCDC No. 2008263, F = $C_{27}H_{33}N_7O_4$, M = 519.60, T = 296(2) K, space group = $P2_12_12_1$, a = 10.3677(3), b = 11.6016(3), c = 23.4291(6), α = 90°, β = 90°, γ = 90°, V = 2818.10(13) Å^3, Z = 4, μ = 0.085 mm^{-1}, D = 1.225 g cm^{-3}, F(000) = 1104, reflections total = 6999, reflections gathered = 4453, R_{int} = 0.0383, $R_1(F)$ = 0.0628, w$R_2(F^2)$ = 0.1756, S = 1.021, N_{par} = 352.

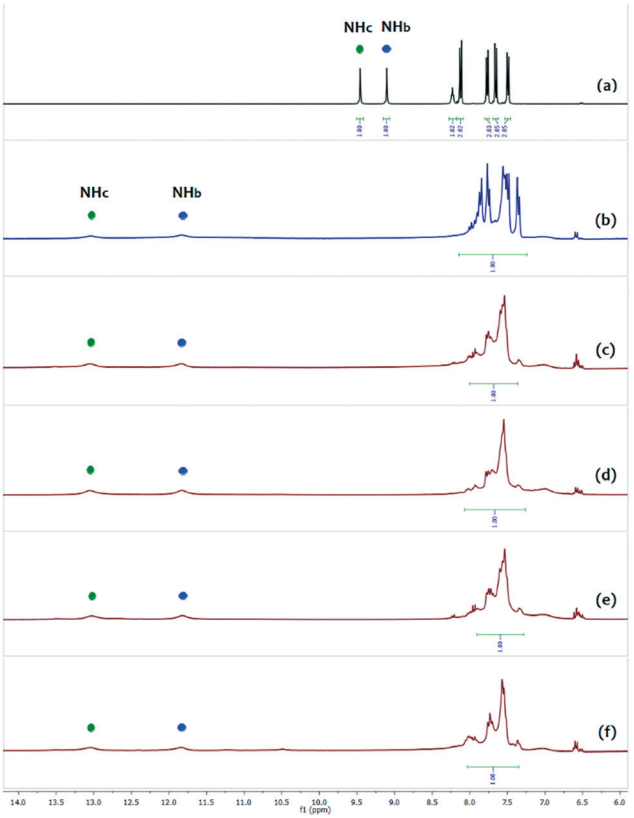

Fig. 4 Aromatic region (6–14 ppm) of ^{1}H-NMR spectra in DMSO-d_6 of (a) **AUL**, (b) hydrogenphosphate complex [(n-Bu_4N)$_2$(**AUL**·HPO_4)·DMSO·CH_3CN] and hydrogenphosphate complex of **AUL** obtained from phosphate extraction experiments (dichloromethane/water) in the presence of (c) (n-Bu_4N^+)F^-, (d) (n-Bu_4N^+)CH_3COO^-, (e) (n-Bu_4N^+)OH^- and (f) (n-Bu_4N^+)F^- in the organic phase and Na_2SO_4 in the aqueous phase (all spectra recorded are provided in Fig. S24–S30 in the ESI†).

HPO_4^{2-} in the solid state and not with any of the other tested anions (F^-, Cl^-, CN^-, CH_3COO^- and HSO_4^-).

Single crystal X-ray structures

Single crystal X-ray analysis of the hydrogenphosphate complex with **AUL** yielded the crystal composition (n-Bu_4N)$_2$(**AUL**·HPO_4)·DMSO·CH_3CN. In the solid state, the HPO_4^{2-} anion is encapsulated within the tripodal cavity by six strong charge-assisted hydrogen bonds[16] (average N···O–P = 2.820 Å) donated from the three urea groups (Fig. 3a, Table S2 in the ESI†). Two n-Bu_4N^+ cations are present in the crystal lattice together with two solvent molecules (DMSO and CH_3CN). The anion complex crystallized in the triclinic $P\bar{1}$ space group from the DMSO–CH_3CN mixture at room temperature. The slightly longer P–O1 bond of 1.602(3) Å compared to the other P–O bonds of 1.513(3) to 1.522(3) Å suggest that the H atom resides on O1 and is not delocalized over the phosphate group.[16b] The presence of two n-Bu_4N^+ cations in the asymmetric unit further confirmed the presence of a hydrogenphosphate dianion, HPO_4^{2-}, in the crystal structure. Two encapsulated HPO_4^{2-} anions are observed to be in dimeric association by complementary O–H···O hydrogen bonds (P–O···O–P = 2.594 Å) resulting in the formation of a dimeric capsular assembly (Fig. 3b).[17] Two amide groups are involved in an intramolecular N–H···O=C hydrogen bond (N···O = 3.031 Å) and the third amide –NH is involved in intermolecular N–H···O=S hydrogen bonding (N···O = 2.984 Å) with the lattice DMSO molecule (Fig. 3a). The lattice CH_3CN molecule forms a weak C–H···O hydrogen bond with a phosphate oxygen (C···O–P = 3.421 Å). The n-Bu_4N^+ cations are also involved in weak C–H···O interactions with two amide (O=C–NH) groups and two nitro ($–NO_2$) groups of **AUL** (Fig. S46 in the ESI†). Thus, several strong hydrogen bond interactions stabilize a HPO_4^{2-} anion within the tripodal urea cavity supported by a number of weak C–H hydrogen bond interactions in the crystal lattice.

All three samples of single crystals of **AUL**·2DMSO obtained in the presence of fluoride, chloride and acetate (n-Bu_4N^+ salts) from DMSO–CH_3CN solutions were found to show identical cell parameters. Powder X-ray diffraction patterns of the bulk samples were also observed to be identical (Fig. S44 in the ESI†). Single crystal structural elucidation revealed that **AUL** crystallized in the triclinic $P\bar{1}$ space group with two DMSO molecules in the crystal lattice (Fig. 3c). Two urea groups of **AUL** are hydrogen bonded to two DMSO molecules of the lattice while the third urea group is hydrogen bonded to the carbonyl oxygen of two adjacent receptor units. One lattice DMSO was observed to be disordered over two positions and in order to model this disorder, a PART command was used with 0.6 (60%) and 0.4 (40%) contributions for the two fractions.[18] The amide groups of **AUL** are involved in the strong intramolecular N–H···O=C hydrogen bond (N···O = 3.031 Å), as observed in the structure of the hydrogenphosphate complex.

An intramolecular N–H···O=C hydrogen bond (N···O = 3.020 Å) between two amide groups has also been observed in the X-ray structure of **AL**·H_2O (**AL** is the amine precursor of **AUL** and **AAL** in Scheme 1), which crystallized from ethanol (Fig. 3d). Both **AUL**·2DMSO and **AL**·H_2O also showed intermolecular N–H···O=C hydrogen bond (N···O = 2.907 Å and 2.930 Å respectively) formation between the third amide –NH and an amide carbonyl oxygen of the adjacent tripodal unit (Fig. S47 in the ESI†).

Thus, crystal structures of both **AUL**·2DMSO and (n-Bu_4N)$_2$(**AUL**·HPO_4)·DMSO·CH_3CN showed the presence of an intramolecular N–H···O=C hydrogen bond between two amide groups, which induces conformational rigidity and restricts the flexibility of the two tripodal arms to encapsulate anions of different sizes and shapes. The urea groups are however free to rotate by the aryl-urea C–NH single bonds, as observed in the crystal structures. The intramolecular N–H···O=C hydrogen bond is inherent to **AUL** and its HPO_4^{2-} complex, since this has also been observed in the structure of hydrated **AL** which yielded **AUL** upon the reaction with 4-nitrophenyl isocyanate. Thus, selective encapsulation of HPO_4^{2-} by **AUL** is possibly due to receptor–anion

complementarity *i.e.*, the receptor cavity size and acidity of urea –NH protons of **AUL** complement the geometry (size/shape) and basicity of the HPO_4^{2-} anion.

On the other hand, the intramolecular N–H···O═C hydrogen bond between the amide groups is perhaps missing in the solution state because the ^{1}H-NMR spectrum of **AUL** indicated that the three tripodal arms are equivalent. Formation of the intramolecular N–H···O═C hydrogen bond between the amide groups would have disrupted the C_{3v} symmetry in solution and additional peaks could have appeared in the ^{1}H-NMR spectrum of **AUL** for the nonequivalent tripodal arms. The absence of intramolecular hydrogen bonding provides conformational flexibility to the tripodal arms which could reorganize and adjust their cavity size to encapsulate anions of different sizes and shapes by hydrogen bonds. This is the reason why significant broadening and/or downfield shifts of the urea –NH signals have been observed due to dynamic anion coordination in the ^{1}H-NMR spectra of **AUL** in the presence of several anions (F^-, Cl^-, CN^-, CH_3COO^-, $H_2PO_4^-$ and HSO_4^- supplied as quaternary ammonium salts). Meanwhile, in the crystallization experiments formation of the intramolecular N–H···O═C hydrogen bond between the amide groups plays a pivotal role in selective recognition of hydrogenphosphate.

Binding energy calculations of receptor–anion complexes

In order to further gain insight into the selective binding of the hydrogenphosphate dianion by **AUL** over other competitive anions, we have carried out binding energy calculations based on density functional theory (DFT). Energy optimization was carried out using the hybrid density functional theory incorporating the B97D correlation functional *via* Kohn–Sham self-consistent theory calculations employing the NWChem program.[19] The 6-31G(d,p) basis set was used for all computations and obtained using the EMSL Basis Set Library.[20]

To calculate the binding energy of **AUL** with anions such as F^-, CN^-, CH_3COO^-, HSO_4^-, SO_4^{2-} and HPO_4^{2-}, energy optimization of the receptor and anion was performed to obtain hydrogen-bonded complexes of **AUL** with each anion (Fig. S23 in the ESI†). Further, energy optimization of the free receptor conformer and free anion was carried out independently to calculate the binding energy (B.E.) using the equation B.E. = $(E_{receptor} + E_{anion}) - E_{complex}$ in Hartree (1 Hartree = 2625.5 kJ mol^{-1}).[13e] DFT calculations revealed that the binding affinity of **AUL** for HPO_4^{2-} is the highest followed by fluoride, acetate, cyanide and hydrogen sulfate. The binding energy of **AUL** for HPO_4^{2-} (1063 kJ mol^{-1}) is nearly double as compared to HSO_4^- (483 kJ mol^{-1}) and CN^- (538 kJ mol^{-1}), and higher as compared to F^- (768 kJ mol^{-1}) and CH_3COO^- (761 kJ mol^{-1}) (Table S1 in the ESI†). Calculations have also been carried out with the sulfate (SO_4^{2-}) dianion, revealing that the binding affinity of **AUL** for SO_4^{2-} (1018 kJ mol^{-1}) is marginally lower than HPO_4^{2-} (1063 kJ mol^{-1}). However, extraction experiments have proven that **AUL** (mixed with n-Bu_4NF in dichloromethane) can selectively extract and encapsulate the HPO_4^{2-} dianion from an aqueous solution mixture of phosphate and sulfate (see below). Thus, it can be argued that dimeric association between HPO_4^{2-} ions resulting in the formation of a hydrogen bonded capsular assembly (Fig. 3b) is possibly responsible for the observed selectivity of **AUL** for HPO_4^{2-}.[21] Such a dimer formation is not possible in the case of SO_4^{2-}, while HSO_4^- showed the least affinity for **AUL** (483 kJ mol^{-1}).

Energy optimization of **AUL** with the PO_4^{3-} anion to obtain the hydrogen-bonded complex showed deprotonation of two urea –NH by PO_4^{3-} to form $H_2PO_4^-$. The binding energy of the deprotonated receptor–phosphate hydrogen bonded complex was calculated to be 2261 kJ mol^{-1}. However, such a deprotonated receptor–anion complex is ideally not possible to obtain from crystallization experiments since the deprotonated receptor crystallizes with counter-cations present in the solution.[13c,d] Thus, we have been able to validate the selective binding of HPO_4^{2-} by **AUL** in the crystallization experiments based on theoretical calculations.

Extraction of hydrogenphosphate from water

The selective encapsulation of HPO_4^{2-} by **AUL** has encouraged us to achieve extraction of HPO_4^{2-} from water in the presence of competitive anions. In a typical liquid–liquid extraction experiment, **AUL** (100 mg) was dissolved in dichloromethane (20 mL DCM) in the presence of two equivalents $(n\text{-}Bu_4N^+)F^-$ or $(n\text{-}Bu_4N^+)CH_3COO^-$ or $(n\text{-}Bu_4N^+)OH^-$ and an aqueous solution of potassium phosphate (5 equivalents of K_3PO_4 dissolved in 10 mL water) was added into the DCM solution. The solution mixture was then stirred at room temperature for about an hour and the DCM layer was separated from the aqueous layer and treated with anhydrous sodium sulfate. The solution was then filtered and evaporated to dryness to obtain a yellow powder that was dissolved in DMSO-d_6 and characterized by ^{1}H-NMR and ^{31}P-NMR analysis (Fig. S24–S28 in the ESI†).

^{1}H-NMR and ^{31}P-NMR spectra of the compounds obtained from extraction experiments closely resemble the spectra of the hydrogenphosphate complex $[(n\text{-}Bu_4N)_2(\mathbf{AUL}\cdot HPO_4)\cdot DMSO\cdot CH_3CN]$ (Fig. 4b–e). Notably, the chemical shift of the urea –NH signals (–NH_b at 11.90 and –NH_c at 13.10 ppm) and the integral values of the aromatic –CH peaks and tetrabutylammonium peaks are observed to be similar in all spectra obtained (Fig. 4be– and S24–28 in the ESI†). It is to be noted that tetrabutylammonium salts of Cl^-, Br^-, Br_3^-, NO_3^- and HSO_4^- are not capable of dissolving **AUL** in DCM due to their weakly basic nature.

In a control experiment, an aqueous solution of K_3PO_4 was treated with a DCM solution mixture of **AUL** and $(n\text{-}Bu_4N^+)H_2PO_4^-$ to obtain a phosphate complex from the organic phase. The ^{1}H-NMR spectrum of the isolated phosphate complex is comparable to the spectra of the above extracted samples (Fig. 4c–e) suggesting the exclusive

formation of the HPO_4^{2-} complex in the extraction experiments (Fig. S32 in the ESI†).

In another experiment, **AUL** (100 mg) was dissolved in dichloromethane (20 mL) in the presence of two equivalents of (n-Bu_4N^+)F^- and an aqueous solution mixture of potassium phosphate and sodium sulfate (5 equivalents of each salt dissolved in 10 mL water) was added into the DCM solution. The solution mixture was then stirred for about an hour and the DCM layer was separated from the aqueous layer. The ^{1}H-NMR and ^{31}P-NMR (in DMSO-d_6) spectra of the compound isolated from the DCM layer were observed to be identical to the other extracted samples of the hydrogenphosphate complex (Fig. 4f and Fig. S29–30 in the ESI†). The FT-IR spectrum of the isolated compound also matches perfectly with the sample extracted in the presence of only (n-Bu_4N^+)F^- (Fig. S31 in the ESI†).

It is important to mention that $H_2PO_4^-$ and HPO_4^{2-} exist in equilibrium ($H_2PO_4^- \leftrightarrows HPO_4^{2-}$) at neutral pH (p$K_a$ 7.21), while PO_4^{3-} can exist only under strongly basic conditions (pK_a 12.67) in aqueous medium.[22] Thus, in spite of the fact that a PO_4^{3-} salt (K_3PO_4) was used in the extraction experiment, we have isolated a HPO_4^{2-} complex of **AUL** from the organic layer. It is remarkable to note that extraction of HPO_4^{2-} from water occurs so efficiently with **AUL** by exchange of competitive anions (such as F^-, OH^- or CH_3COO^-) with HPO_4^{2-} between the two immiscible phases, indicating the very high affinity of **AUL** for HPO_4^{2-}.

Anion binding studies of amide-based receptor AAL

Similar to the urea group, the amide –NH protons are also strong hydrogen bond donors and several amide-based receptors are known to form stable hydrogen-bonded complexes with halides and oxo-anions.[2,4] The ^{1}H-NMR spectrum of **AAL** in DMSO-d_6 showed an amide –NH signal (–NH_b) at 10.68 ppm, while the other –NH signal (–NH_a) has merged with the aromatic –CH peak at 8.32 ppm, as evident from the NMR integral values (Fig. 5a and Fig. S6 in the ESI†). Aromatic –CH proton signals of the peripheral nitrophenyl ring appeared as two doublets (at 8.12 and 8.32 ppm), and the inner benzamide –CH protons appeared as a singlet (at 7.82 ppm) due to amide group substitution at the *para* positions (Fig. 5a). Addition of n-Bu_4N^+ or Et_4N^+ salts of F^-, CN^-, CH_3COO^- and $H_2PO_4^-$ to individual solutions of **AAL** (in DMSO-d_6) resulted in disappearance of the amide –NH_b signal due to dynamic anion coordination between the amide groups and added anion (Fig. 5). Addition of (n-Bu_4N^+)Cl^- resulted in a negligible downfield shift of the amide –NH_b signal (Fig. 5c). Due to receptor–anion hydrogen bond interactions, changes have also been observed for the aromatic –CH proton signals in the presence of F^-, Cl^-, CN^-, CH_3COO^- and $H_2PO_4^-$ anions (Fig. 5). However, addition of n-Bu_4N^+ salts of Br^-, Br_3^-, NO_3^-, and HSO_4^- to solutions of **AAL** (in DMSO-d_6) did not show any observable shift of –NH_b and –CH signals, suggesting that the receptor did not interact well with these anions in solution (Fig. 5). Thus, in order to obtain hydrogen-bonded anion complexes in the solid state, we have crystallized **AAL** in the presence of n-Bu_4N^+ or Et_4N^+ salts of F^-, CN^-, CH_3COO^- and $H_2PO_4^-$ in the DMSO–CH_3CN (8 : 2 v/v) solvent mixture.

No single crystals were formed from any of the above solution mixtures containing **AAL** and a quaternary ammonium salt. Instead, yellow crystalline powders were precipitated in each case which were then collected by filtration and washed repeatedly with methanol for subsequent analysis. ^{1}H-NMR analysis (in DMSO-d_6) revealed the absence of a n-Bu_4N^+ or Et_4N^+ cation in these precipitated

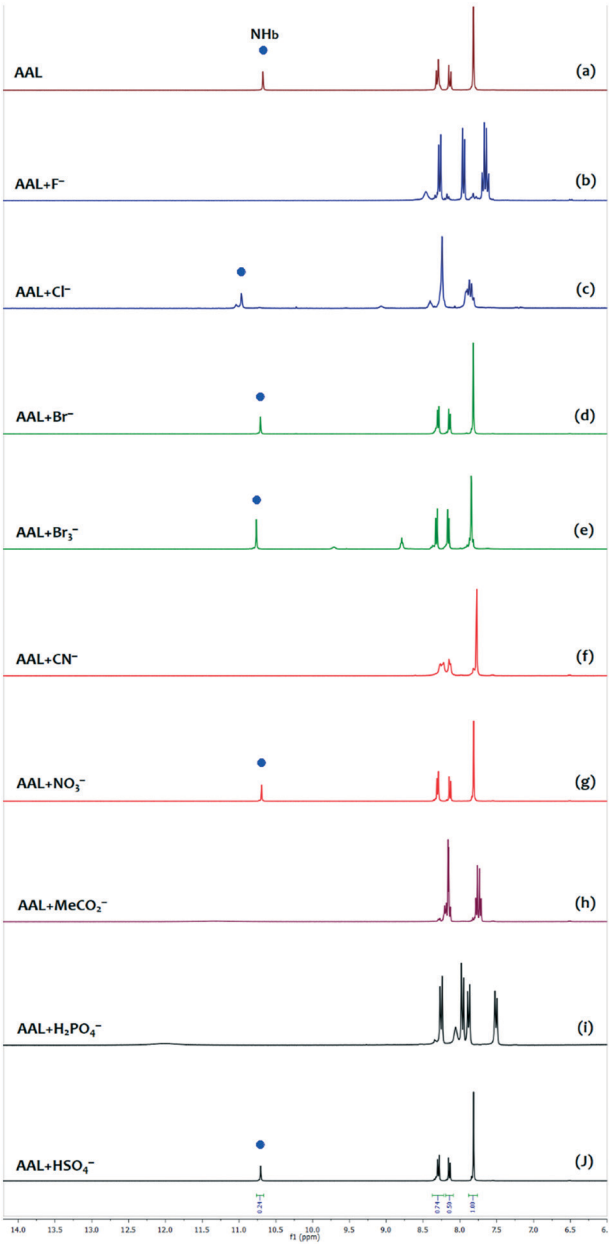

Fig. 5 Aromatic region (6–14 ppm) of ^{1}H-NMR (DMSO-d_6) spectra of (a) **AAL** and in the presence of (b) (n-Bu_4N^+)F^-, (c) (n-Bu_4N^+)Cl^-, (d) (n-Bu_4N^+)Br^-, (e) (n-Bu_4N^+)Br_3^-, (f) (Et_4N^+)CN^-, (g) (n-Bu_4N^+)NO_3^-, (h) $Li^+CH_3COO^-$, (i) (n-Bu_4N^+)$H_2PO_4^-$, and (j) (n-Bu_4N^+)HSO_4^-, (full spectra are provided in Fig. S34–S42 in the ESI†).

compounds and the spectrum in each case matches perfectly with the **AAL** spectrum in DMSO-d_6 (Fig. S43 in the ESI†). It is thus confirmed that no hydrogen bonded receptor–anion complex was formed from the crystallization experiments and the neat receptor has precipitated out in all cases. The powder X-ray diffraction patterns of all the samples were identical (Fig. S45 in the ESI†). The inefficiency of **AAL** to form a hydrogen-bonded complex in the solid state can be explained by the lack of sufficient hydrogen bond donor atoms to stabilize an anion within the receptor cavity, *i.e.*, lack of receptor–anion complementarity where the cavity size of the receptor also plays a critical role in anion recognition.

Conclusion

In conclusion, we have achieved selective encapsulation of the hydrogenphosphate dianion by a second generation tripodal urea-based receptor (**AUL**). Crystallization of **AUL** in the presence of various anions (supplied as n-Bu_4N^+/Et_4N^+ salts) yielded **AUL**–2DMSO adducts except from the solution containing $H_2PO_4^-$ which formed a hydrogen-bonded anion complex (n-Bu_4N)$_2$(**AUL**·HPO_4)·DMSO·CH_3CN due to receptor–anion complementarity. The selectivity of **AUL** for hydrogenphosphate has also been reflected in the extraction experiments where HPO_4^{2-} could easily be extracted into the organic layer (dichloromethane) from water (K_3PO_4 solution) by anion exchange between the two phases. Theoretical calculations on energy optimized hydrogen bonded receptor–anion complexes also showed the highest binding affinity of **AUL** for the HPO_4^{2-} anion. The differences in solid and solution state anion binding affinities are due to the formation of the intramolecular N–H···O═C hydrogen bond between the receptor side arms (during crystallization) which dictate the cavity size and hence the anion complementarity of the receptor having urea groups as hydrogen bond donors. Most importantly, this work showcases the synthetic modification of a first generation tripodal receptor into an anion selective second-generation receptor and unfolds the numerous possibilities of obtaining anion selectivity by mere structural alteration of known hydrogen bond donor receptors.

Conflicts of interest

There are no conflicts to declare.

Acknowledgements

SKD acknowledges the Department of Science and Technology (DST) under the Ministry of Science and Technology India, for providing financial support through the INSPIRE Faculty award (DST/INSPIRE/04/2016/001867). We thank DST-FIST for providing single crystal X-ray diffraction and NMR facilities at the School of Chemical Sciences, Goa University. SKD and CJ thank the Alexander von Humboldt Foundation, Germany, for providing the opportunity for research collaboration.

Notes and references

1 (*a*) K. Bowman-James, *Acc. Chem. Res.*, 2005, **38**, 671–678; (*b*) S. Kubik, *Chem. Soc. Rev.*, 2009, **38**, 585–605; (*c*) V. Amendola, D. Esteban-Gomez, L. Fabbrizzi and M. Licchelli, *Acc. Chem. Res.*, 2006, **39**, 343–353; (*d*) K. M. Mullen and P. D. Beer, *Chem. Soc. Rev.*, 2009, **38**, 1701–1713; (*e*) P. A. Gale, *Chem. Commun.*, 2008, 4525–4540; (*f*) B. P. Hay, *Chem. Soc. Rev.*, 2010, **39**, 3700–3708; (*g*) G. Cavallo, P. Metrangolo, T. Pilati, G. Resnati, M. Sansotera and G. Terraneo, *Chem. Soc. Rev.*, 2010, **39**, 3772–3783; (*h*) J. T. Davis, O. Okunolaa and R. Quesada, *Chem. Soc. Rev.*, 2010, **39**, 3843–3862; (*i*) A.-F. Li, J.-H. Wang, F. Wang and Y.-B. Jiang, *Chem. Soc. Rev.*, 2010, **39**, 3729–3745; (*j*) C. Jia, W. Zuo, D. Zhang, X.-J. Yang and B. Wu, *Chem. Commun.*, 2016, **52**, 9614–9627.

2 (*a*) S. Peng, Q. He, G. I. Vargas-Zúñiga, L. Qin, I. Hwang, S. K. Kim, N. J. Heo, C.-H. Lee, R. Dutta and J. L. Sessler, *Chem. Soc. Rev.*, 2020, **49**, 865–907; (*b*) S. K. Kim and J. L. Sessler, *Chem. Soc. Rev.*, 2010, **39**, 3784–3809; (*c*) M. Wenzel, J. R. Hiscock and P. A. Gale, *Chem. Soc. Rev.*, 2012, **41**, 480–520; (*d*) P. A. Gale, S. E. García-Garrido and J. Garric, *Chem. Soc. Rev.*, 2008, **37**, 151–190; (*e*) D. Mungalpara, A. Valkonen, K. Rissanen and S. Kubik, *Chem. Sci.*, 2017, **8**, 6005–6013; (*f*) S. Kubik, *Chem. Soc. Rev.*, 2010, **39**, 3648–3663; (*g*) S. O. Kang, J. M. Llinares, V. W. Day and K. Bowman-James, *Chem. Soc. Rev.*, 2010, **39**, 3980–4003; (*h*) R. Dutta and P. Ghosh, *Chem. Commun.*, 2014, **50**, 10538–10554.

3 (*a*) R. Custelcean, P. Remy, P. V. Bonnesen, D. Jiang and B. A. Moyer, *Angew. Chem., Int. Ed.*, 2008, **47**, 1866–1869; (*b*) R. Custelcean, B. A. Moyer and B. P. Hay, *Chem. Commun.*, 2005, 5971–5974; (*c*) S. K. Dey and G. Das, *Dalton Trans.*, 2012, **41**, 8960–8972; (*d*) J. Zhao, D. Yang, Y. Zhao, L. Cao, Z. Zhang, X.-J. Yang and B. Wu, *Dalton Trans.*, 2016, **45**, 7360–7365; (*e*) I. Basaran, M. E. Khansari, A. Pramanik, B. M. Wong and M. A. Hossain, *Tetrahedron Lett.*, 2014, **55**, 1467–1470; (*f*) S. K. Dey and G. Das, *Chem. Commun.*, 2011, **47**, 4983–4985; (*g*) A. S. Singh and S.-S. Sun, *J. Org. Chem.*, 2012, **77**, 1880–1890; (*h*) D. P. Cormode, S. S. Murray, A. R. Cowley and P. D. Beer, *Dalton Trans.*, 2006, 5135–5140; (*i*) N. Singh and D. O. Jang, *Org. Lett.*, 2007, **9**, 1991–1994; (*j*) L. Qin, A. Hartley, P. Turner, R. B. P. Elmes and K. A. Jolliffe, *Chem. Sci.*, 2016, **7**, 4563–4572; (*k*) C. J. Woods, S. Camiolo, M. E. Light, S. J. Coles, M. B. Hursthouse, M. A. King, P. A. Gale and J. W. Essex, *J. Am. Chem. Soc.*, 2002, **124**, 8644–8652; (*l*) P. G. Young and K. A. Jolliffe, *Org. Biomol. Chem.*, 2012, **10**, 2664–2672; (*m*) I. Ravikumar and P. Ghosh, *Chem. Commun.*, 2010, **46**, 6741–6743.

4 (*a*) S. K. Dey, A. Basu, R. Chutia and G. Das, *RSC Adv.*, 2016, **6**, 26568–26589; (*b*) M. Arunachalam and P. Ghosh, *Chem. Commun.*, 2011, **47**, 8477–8492.

5 (*a*) I. Ravikumar and P. Ghosh, *Chem. Soc. Rev.*, 2012, **41**, 3077–3098; (*b*) R. Ghosh, T. K. Ghosh and P. Ghosh, *Dalton Trans.*, 2020, **49**, 3093–3097; (*c*) S. Chakraborty, R. Dutta and P. Ghosh, *Chem. Commun.*, 2015, **51**, 14793–14796; (*d*) I. Ravikumar, S. Saha and P. Ghosh, *Chem. Commun.*, 2011, **47**,

4721–4723; (*e*) R. Custelcean and P. Remy, *Cryst. Growth Des.*, 2009, **9**, 1985–1990; (*f*) C. Jia, B. Wu, S. Li, X. Huang, Q. Zhao, Q.-S. Li and X.-J. Yang, *Angew. Chem., Int. Ed.*, 2011, **50**, 486–489; (*g*) J. Almog, I. Gavish-Abramovich, R. Rozin, S. Cohen, G. Yardeni and I. Zilbermann, *Eur. J. Inorg. Chem.*, 2012, 4427–4432; (*h*) C. R. Rice, C. Slater, R. A. Faulkner and R. L. Allan, *Angew. Chem., Int. Ed.*, 2018, **57**, 13071–13075; (*i*) B. Akhuli and P. Ghosh, *Chem. Commun.*, 2015, **51**, 16514–16517; (*j*) S. Chakraborty, R. Dutta and P. Ghosh, *Chem. Commun.*, 2015, **51**, 14793–14796.

6 (*a*) K. E. Havens and C. L. Schelske, *Environ. Pollut.*, 2001, **113**, 1–9; (*b*) M. F. Coveney, E. F. Lowe, L. E. Battoe, E. R. Marzolf and R. Conrow, *Freshwater Biol.*, 2005, **50**, 1718–1730; (*c*) C. L. Schelske, E. F. Stoermer and W. F. Kenney, *Limnol. Oceanogr.*, 2006, **51**, 728–748.

7 A. M. Hyde, S. L. Zultanski, J. H. Waldman, Y.-L. Zhong, M. Shevlin and F. Peng, *Org. Process Res. Dev.*, 2017, **21**, 1355–1370.

8 (*a*) N. Busschaert, C. Caltagirone, W. Van Rossom and P. A. Gale, *Chem. Rev.*, 2015, **115**, 8038–8155; (*b*) Z. Wang, H. Luecke, N. Yao and F. A. Quiocho, *Nat. Struct. Biol.*, 1997, **4**, 519.

9 (*a*) S. Pal, T. K. Ghosh, R. Ghosh, S. Mondal and P. Ghosh, *Coord. Chem. Rev.*, 2020, **405**, 213128and references therein; (*b*) D. Yang, J. Zhao, X.-J. Yang and B. Wu, *Org. Chem. Front.*, 2018, **5**, 662–690; (*c*) C. Bazzicalupi, A. Bencini and V. Lippolis, *Chem. Soc. Rev.*, 2010, **39**, 3709–3728; (*d*) M. V. R. Raju, S. M. Harris and V. C. Pierre, *Chem. Soc. Rev.*, 2020, **49**, 1090–1108.

10 X. Huang, B. Wu, C. Jia, B. P. Hay, M. Li and X.-J. Yang, *Chem. – Eur. J.*, 2013, **19**, 9034–9041.

11 I. Ravikumar, P. S. Lakshminarayanan and P. Ghosh, *Inorg. Chim. Acta*, 2010, **363**, 2886–2895.

12 Most tetrabutylammonium (n-Bu_4N^+) or tetraethylammonium (Et_4N^+) salts are hygroscopic in nature and thus, weighing identical equivalents of each salt relative to **AUL/AAL** was hard to achieve.

13 (*a*) J. W. Steed and J. L. Atwood, *Supramolecular Chemistry*, Wiley, New York, 2nd edn, 2000; (*b*) S. K. Dey and G. Das, *Dalton Trans.*, 2011, **40**, 12048–12051; (*c*) N. Busschaert, M. Wenzel, M. E. Light, P. Iglesias-Hernandez, R. Perez-Tomas and P. A. Gale, *J. Am. Chem. Soc.*, 2011, **133**, 14136–14145; (*d*) A. Basu, S. K. Dey and G. Das, *RSC Adv.*, 2013, **3**, 6596–6605; (*e*) M. E. Khansari, M. H. Hasan, C. R. Johnson, N. A. Williams, B. M. Wong, D. R. Powell, R. Tandon and M. A. Hossain, *ACS Omega*, 2017, **2**, 9057–9066.

14 Commercially available tetrabutylammonium (n-Bu_4N^+) acetate (Sigma-Aldrich) was received as a thick sticky liquid due to its hygroscopic nature and thus, lithium acetate (soluble in DMSO-d_6) was used for the ^{1}H-NMR experiment as a source for the acetate anion.

15 (*a*) R. Chutia, S. K. Dey and G. Das, *Cryst. Growth Des.*, 2015, **15**, 4993–5001; (*b*) R. Chutia, S. K. Dey and G. Das, *Cryst. Growth Des.*, 2013, **13**, 883–892; (*c*) P. S. Lakshminarayanan, I. Ravikumar, E. Suresh and P. Ghosh, *Chem. Commun.*, 2007, 5214–5216.

16 (*a*) A. Tahli, Ü. Köc, R. F. M. Elshaarawy, A. C. Kautz and C. Janiak, *Crystals*, 2016, **6**, 23; (*b*) C. Heering, B. Nateghi and C. Janiak, *Crystals*, 2016, **6**, 22; (*c*) B. G. Hernández, J. K. Maclaren, H. A. Höppe, J. Pasán, J. Sanchiz and C. Janiak, *CrystEngComm*, 2012, **14**, 2635–2644; (*d*) J. K. Maclaren and C. Janiak, *Inorg. Chim. Acta*, 2012, **389**, 183–190; (*e*) B. M. Drašković, G. A. Bogdanović, M. A. Neelakantan, A.-C. Chamayou, S. Thalamuthu, Y. S. Avadhut, J. S. auf der Günne, S. Banerjee and C. Janiak, *Cryst. Growth Des.*, 2010, **10**, 1665–1676; (*f*) B. Wu, X. Huang, Y. Xia, X.-J. Yang and C. Janiak, *CrystEngComm*, 2007, **9**, 676–685; (*g*) M. D. Ward, *Chem. Commun.*, 2005, 5838–5842.

17 (*a*) K. Pandurangan, J. A. Kitchen, S. Blasco, E. M. Boyle, B. Fitzpatrick, M. Feeney, P. E. Kruger and T. Gunnlaugsson, *Angew. Chem., Int. Ed.*, 2015, **54**, 4566–4569; (*b*) P. S. Lakshminarayanan, I. Ravikumar, E. Suresh and P. Ghosh, *Chem. Commun.*, 2007, 5214–5216; (*c*) Y. Zhang, R. Zhang, Y. Zhao, L. Ji, C. Jia and B. Wu, *New J. Chem.*, 2013, **37**, 2266–2270; (*d*) M. Wei, B. Wu, L. Zhao, H. Zhang, S. Li, Y. Zhao and X.-J. Yang, *Org. Biomol. Chem.*, 2012, **10**, 8758–8761.

18 L. J. Farrugia, *J. Appl. Crystallogr.*, 2012, **45**, 849–854.

19 M. Valiev, E. J. Bylaska, N. Govind, K. Kowalski, T. P. Straatsma, H. J. J. Van Dam, D. Wang, J. Nieplocha, E. Apra, T. L. Windus and W. A. de Jong, *Comput. Phys. Commun.*, 2010, **181**, 1477–1489.

20 K. L. Schuchardt, B. T. Didier, T. Elsethagen, L. Sun, V. Gurumoorthi, J. Chase, J. Li and T. L. Windus, *J. Chem. Inf. Model.*, 2007, **47**, 1045–1052.

21 (*a*) X. Wu, A. M. Gilchrist and P. A. Gale, *Chem*, 2020, **6**, 1296–1309; (*b*) Q. He, P. Tu and J. L. Sessler, *Chem*, 2018, **4**, 46–93.

22 E. A. Katayev, Y. A. Ustynyuk and J. L. Sessler, *Coord. Chem. Rev.*, 2006, **250**, 3004–3037.

